Chemical Engineering Journal 95 (2003) 143–154

Chemical Engineering Journal

www.elsevier.com/locate/cej

A generalized shrinking core model applied to batch adsorption

Pravat Ranjan Jena, Sirshendu De, Jayanta Kumar Basu*

Department of Chemical Engineering, Indian Institute of Technology, Kharagpur 721302, India

Abstract

A two resistance mass transfer model for batch adsorption process has been developed which includes a film mass transfer coefficient and an internal effective diffusivity that controls the internal mass transport process based on the pore diffusion mechanism. This model is based on shrinking core formulation for catalytic reaction. The model proposed here is more generalized, can accommodate wide range of initial adsorbate concentration in feed and the nature of the isotherm. The model is solved numerically and optimized using nonlinear parameter estimation technique in order to match with the experimental kinetic data available in the literature [AIChE J. 39 (1993) 2027; AIChE J. 30 (1984) 692; Adsorp. Sci. Technol. 4 (1987) 58]. In this procedure the process parameters, i.e. the external mass transfer coefficient and internal effective diffusivity are determined for a particular system. Using the estimated parameters, a parametric study has been carried out to observe the effects of initial adsorbate concentration, particle size of adsorbent, mass of adsorbent, etc. on the system kinetics.

Keywords: Adsorption; Mass transfer coefficient; Pore diffusion; Internal diffusivity; Shrinking core model

1. Introduction

Adsorption process plays an important role in a number of natural and industrial systems such as fundamental biological studies, separation and purification processes, recovery of chemical compounds, catalysis and waste treatment processes. It can be advantageously substitute for other separation processes and contribute effectively to remove pollutants remaining in solutions.

Adsorption studies in agitated finite batch adsorbers yield important equilibrium and kinetic data useful for further fixed bed studies and for the prediction of industrial adsorber performance. The adsorber design is based on extensive pilot plant scale experiments [4], which supply the design parameters and such design is specific to system conditions. In order to estimate the parameters for wider operating conditions, mathematical modeling of process kinetics is required.

To develop a mathematical model that describes the adsorption dynamics, following information are generally required:

(1) a complete description of equilibrium behavior, i.e. the maximum level of adsorption attained in a sorbent/sorbate system as a function of the sorbate liquid phase concentration;
(2) a mathematical representation of associated rate of adsorption, which is controlled by the resistances within the sorbent particles.

In adsorption, mainly two resistances prevail—the external liquid film resistance and the resistance in the adsorbent particle. The intraparticle diffusion resistance may be neglected for solutes that exhibit strong solid to liquid phase equilibrium solute distribution, in the initial period of operation. However, even for such systems, the above assumption leads to errors that are substantial beyond the first few minutes if the agitation is high [5]. So the both the resistances are important for kinetic study [1–3,6,7].

The external liquid film resistance is characterized by the external liquid film mass transfer coefficient (k_f). The mass transport within the adsorbent particles is assumed to be a pore diffusion [2,8–10] or homogeneous solid diffusion process [1,11–13].

The pore diffusion model outlined in this paper is based on the unreacted shrinking core model [14,15] with pseudo steady-state approximation. This model has mostly been applied to gas–solid noncatalytic reactions [14], but a number of liquid–solid reactions also have been analyzed using this model [16,17]. In the pore diffusion model, there is adsorption of the adsorbate into the pores with a co-current solute distributed all along the pore wall.

The assumptions made in this model are as follows:

(1) Pore diffusivity is independent of concentration.
(2) Adsorption isotherm is irreversible.

* Corresponding author. Tel.: +91-3222-283914; fax: +91-3222-255303.
E-mail address: jkb@che.iitkgp.ernet.in (J.K. Basu).

1385-8947/$ – see front matter © 2003 Elsevier B.V. All rights reserved.
doi:10.1016/S1385-8947(03)00097-4

Nomenclature

A, B	Radke–Prausnitz isotherm constant (l/g)
C_t	liquid phase concentration at time t (mg/l)
C_{et}	equilibrium liquid phase concentration at time t (mg/l)
C_0	initial liquid phase concentration (mg/l)
D_p	effective diffusion coefficient in the adsorbent (m^2/s)
k_f	liquid phase mass transfer coefficient (m/s)
k_p	pore mass transfer coefficient at time t (m/s)
K_0	Langmuir isotherm constant (l/mg)
$N(t)$	adsorption rate at time t (mg/s)
R	adsorbent particle radius (m)
R_f	radius of concentration front (m)
t	time (s)
V	volume of batch reactor (l)
W	weight of the adsorbent (g)
Y_e	solid phase concentration at a particular time t (mg/g)
Y_s	Langmuir isotherm constant (l/g)
$\bar{Y}_t$	average solid phase concentration at time t (mg/g)

Greek letters

α_1	constant used in Fritz–Schlunder isotherm ($mg/g\,(mg/l)^{-\beta_1}$)
α_2	constant used in Fritz–Schlunder isotherm ($(mg/l)^{-\beta_2}$)
β_1, β_2	constants used in Fritz–Schlunder isotherm, dimensionless
δ	Radke–Prausnitz isotherm constant
ρ	adsorbent density (kg/m^3)

Subscripts

f	liquid phase
o	initial
p	pores
t	at time t

Superscript

$*$	non-dimensional

(3) Pseudo steady-state approximation is valid.
(4) The driving force in both film and particle mass transfer is linear.
(5) Adsorbent particles are spherical.

The adsorption kinetic model based on this approach is available in literature [2]. The major limitation of this model [2] is that it is specific to the nature of isotherm. This means that the model available in literature is most suitable for Langmuir type isotherm, i.e. formation of a monolayer of adsorbate on the adsorbent. Besides, this model is only applicable for higher initial adsorbate concentration in solution so that the batch process operating line intercepts the invariant zone of isotherm. For example, for Astrazone Blue Dye on Silica system, the literature model is applicable for $C_0 \gg 200$ mg/l [2]. The present model which is more generalized overcomes the above limitations. The model proposed, here in, can be applied to wide ranges of initial adsorbate concentrations for all possible nature of isotherms. The systems reported here are

(1) The adsorption of Astrazone Blue Dye on Silica (Sorbsil) [2].
(2) The adsorption of *para*-nitrophenol on granular activated carbon from Lurgi [3].
(3) The adsorption of toluene on F300 activated carbon [1].

2. Theory

The present model can accommodate various isotherms. The isotherms for adsorption equilibrium considered are

1. Langmuir isotherm

$$Y_e = \frac{Y_s C_e}{1 + K_0 C_e} \tag{1}$$

2. Fritz–Schlünder isotherm

$$Y_e = \frac{\alpha_1 C_e^{\beta_1}}{1 + \alpha_2 C_e^{\beta_2}} \tag{2}$$

3. Radke–Prausnitz isotherm

$$\frac{1}{Y_e} = \frac{1}{AC_e} + \frac{1}{BC_e^{\delta}} \tag{3}$$

The equations considered for the kinetics of the adsorption process for spherical adsorbent particles for the present model are as follows.

The mass transfer from external liquid phase can be written as

$$N(t) = 4\pi R^2 k_f (C_t - C_{et}) \tag{4}$$

The diffusion of solute through the pores as per Fick's law can be written as

$$N(t) = \frac{4\pi D_p C_{et}}{(1/R_f) - (1/R)} \tag{5}$$

where D_p is the effective diffusivity in the porous adsorbent [18].

The mass balance on a spherical element of adsorbate particle can be written as

$$N(t) = -4\pi R_f^2 Y_{et} \rho \frac{dR_f}{dt} \tag{6}$$

The average concentration on adsorbent particle can be written as

$$\bar{Y}_t = Y_{et}\left[1 - \left(\frac{R_f}{R}\right)^3\right] \tag{7}$$

The differential mass balance over the system by equating the decrease in adsorbate concentration in the solution with

the accumulation of the adsorbate in the adsorbent can be written as

$$N(t) = -V\frac{dC_t}{dt} = W\frac{d\bar{Y}_t}{dt} \tag{8}$$

The dimensionless terms used for simplification are as follows:

$$C_t^* = \frac{C_t}{C_0}, \qquad r = \frac{R_f}{R}, \qquad Bi = \frac{k_f R}{D_p},$$

$$Ch = \frac{W}{VC_0}, \qquad C_{et}^* = \frac{C_{et}}{C_0} \quad \text{and} \quad \tau = \frac{D_p t}{R^2}$$

Simplifying Eqs. (4) and (5)

$$C_{et}^* = \frac{Bi(1-r)C_t^*}{r + Bi(1-r)} = g_i(C_t^*, r) \tag{9}$$

Now differentiating above equation with respect to τ

$$\frac{dC_{et}^*}{d\tau} = \frac{Bi(1-r)}{r + Bi(1-r)}\frac{dC_t^*}{d\tau} - \frac{Bi\, C_t^*}{[r + Bi(1-r)]^2}\frac{dr}{d\tau} \tag{10}$$

From the equilibrium relationship:

$$Y_e(t) = g_2(C_{et}^*) \tag{11}$$

where g_2 is any equilibrium relationship as given in Eqs. (1)–(3).

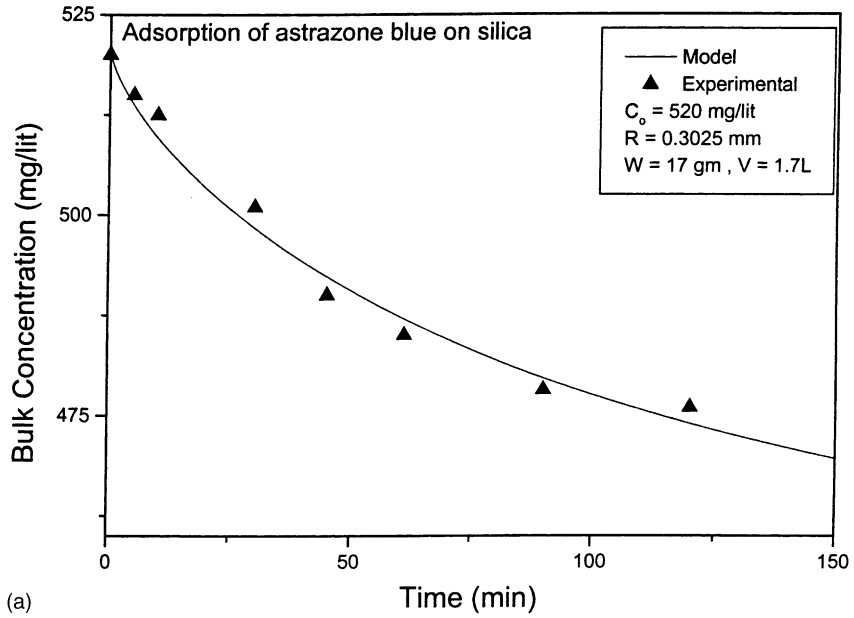

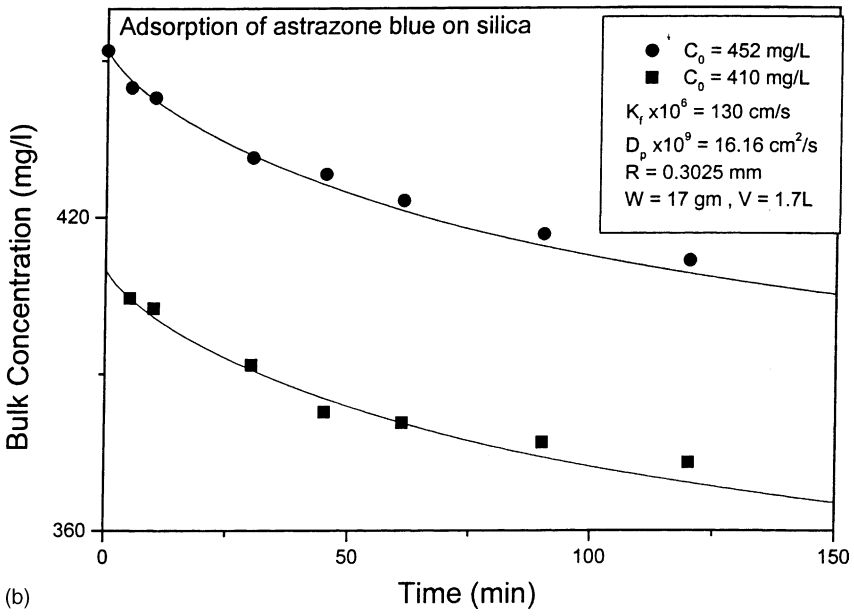

Fig. 1. (a) Adsorption of Astrazone Blue Dye on Silica: (b) effect of initial adsorbate concentration; (c) effect of the mass of adsorbent on concentration decay; (d) effect of silica particle size on concentration decay. Solid lines are the model predictions and symbols are the experimental data.

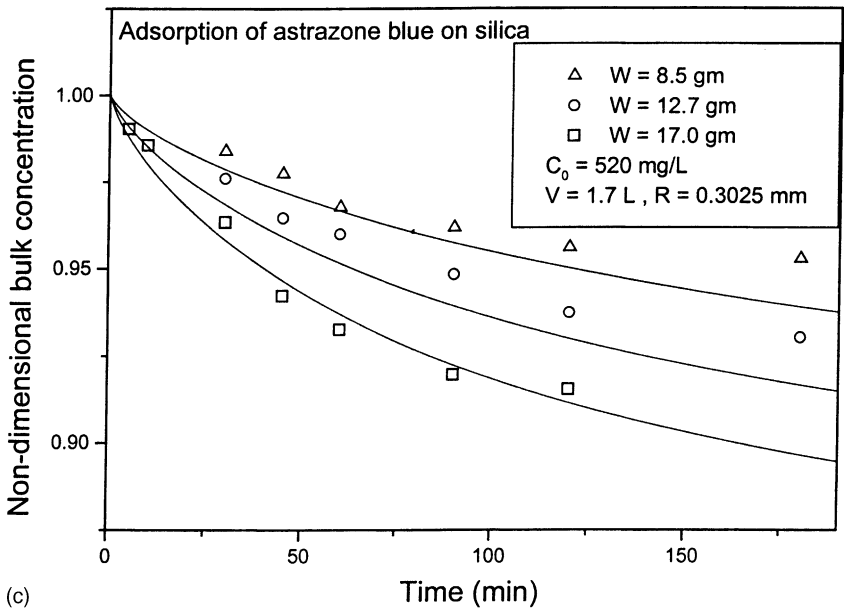

(c)

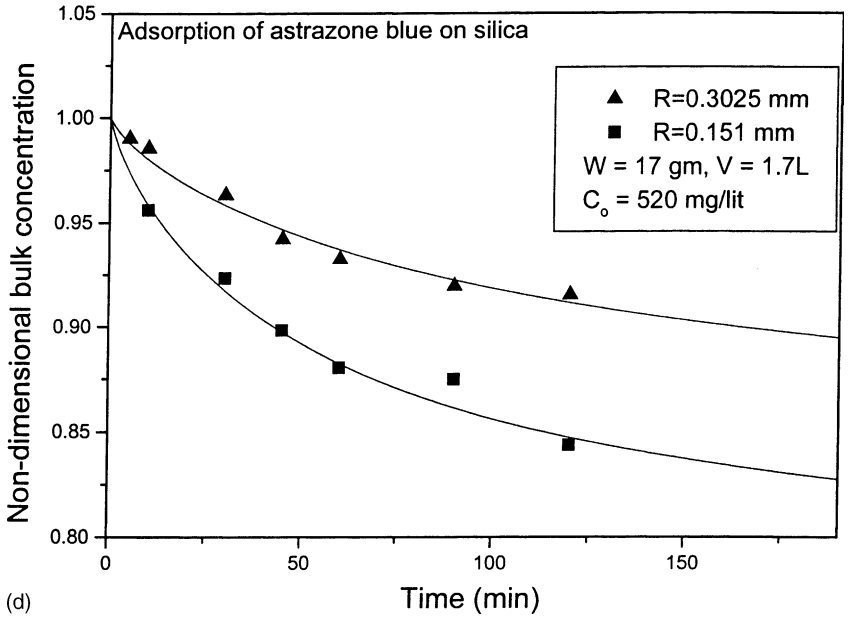

(d)

Fig. 1. (*Continued*).

Simplifying Eqs. (4) and (6)

$$\frac{dr}{d\tau} = \frac{-Bi(C_0/\rho Y_e)(C_t^* - C_{et}^*)}{r^2} \tag{12}$$

Simplifying Eqs. (7) and (8)

$$\frac{dC_t^*}{d\tau} + Ch(1-r^3)\frac{dY_{et}}{d\tau} = 3Ch\,Y_{et}r^2\frac{dr}{d\tau} \tag{13a}$$

For Langmuir isotherm:

$$Y_{et} = \frac{Y_s C_{et}}{1+k_0 C_{et}} = \frac{Y_s C_0 C_{et}^*}{1+k_0 C_0 C_{et}^*} = \frac{Y_{es} C_{et}^*}{1+k_0^* C_{et}^*} \tag{13b}$$

where $Y_{es} = Y_s C_0$ and $k_0^* = k_0 C_0$.

The time derivative of Eq. (13a) becomes

$$\frac{dY_{et}}{d\tau} = \frac{Y_{es}}{(1+k_0^* C_{et}^*)^2}\frac{dC_{et}^*}{d\tau} \tag{14}$$

Combining Eqs. (9), (13a) and (14) and after algebraic manipulation, the following expression is obtained (for Langmuir type isotherm):

$$\frac{dC_t^*}{d\tau} = \frac{N}{M}\frac{dr}{d\tau} \tag{15}$$

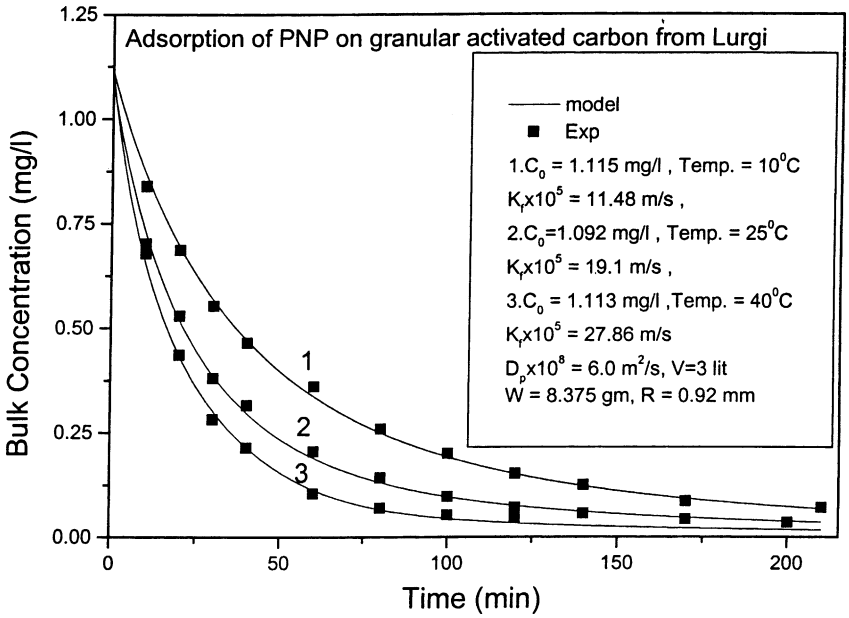

Fig. 2. Effect of temperature on concentration decay.

where

$$M = 1 + Ch(1 - r^3)\frac{Y_{es}\,Bi(1-r)}{(1 + k_0^* C_{et}^*)^2[r + (1-r)Bi]}$$

and

$$N = 3Ch\,Y_{et}r^2 + \frac{Ch\,Y_{es}\,Bi(1-r^3)C_t^*}{(1 + k_0^* C_{et}^*)^2[r + (1-r)Bi]^2}$$

Using Eq. (9), Eq. (12) may be written as

$$\frac{dr}{d\tau} = f_1(C_t^*, r) \tag{16}$$

where

$$f_1 = \frac{-Bi(C_0/\rho Y_e)(C_t^* - C_{et}^*)}{r^2}$$

Using Eqs. (9) and (16), Eq. (15) may be expressed as

$$\frac{dC_t^*}{d\tau} = \frac{N(C_t^*, r)\,f_1(C_t^*, r)}{M(C_t^*, r)} = f_2(C_t^*, r) \tag{17}$$

The initial conditions for Eqs. (16) and (17) are $C_t^* = 1.0$ and $r = 1.0$ at time $\tau = 0.0$. Eqs. (16) and (17) can be solved to find the bulk concentration at any time 't' if we know all the process parameters. The two process parameters, the external mass transfer coefficient (k_f) and internal effective diffusivity (D_p) are unknown to us. These two parameters are estimated by optimizing the experimental concentration profile as outlined in the next section.

3. Numerical analysis

The above set of equations are numerically solved using fourth order Runge–Kutta of step size ($d\tau$) of the order 10^{-5} along with a nonlinear optimization technique (Levenberg–Marquardt) to estimate the two process parameters described above, so that the experimental kinetic profile (i.e. bulk concentration vs. time) is matched. For this purpose, optimization subroutine UNLSF/DUNLSF from IMSL math library has been used.

4. Results and discussion

The adsorption systems studied here encompass—Langmuir isotherm, Radke–Prausnitz isotherm and Fritz–Schlünder isotherm. The systems considered here are (1) Astrazone Blue Dye on Silica, (2) *para*-nitrophenol on granular activated carbon from Lurgi, and (3) toluene on F300 activated carbon. The experimental data on kinetics and the isotherm constants have been reported in literature [1–3]:

Table 1
Radke–Prausnitz isotherm constants

Temperature (°C)	A (l/g)	B (l/g)	δ
10	958.91	2.523	0.195
25	608.16	2.269	0.188
40	315.37	2.078	0.196

Table 2
Model parameters using Radke–Prausnitz isotherm at various temperatures

Temperature (°C)	$k_f \times 10^{-5}$ (m/s)	$D_p \times 10^{-8}$ (m^2/s)
10	11.48	6.0
25	19.10	6.0
40	27.86	6.0

(a) *Langmuir isotherm* [2]: The system is Astrazone Blue Dye on Silica and the isotherm constants are $Y_s = 0.5$ l/g and $K_0 = 0.016$ l/mg. Where Y_e in mg/g and C_e in mg/l. For $W = 17$ g, $V = 1.7$ l, $R = 0.3025$ mm, and $\rho = 2.2$ g/cm^3, the concentration decay data for $C_0 = 520$ mg/l has been used to determine the unknown process parameters using the above numerical procedure as shown in the Fig. 1a. The estimated values of the parameters are as follows: $k_f = 130.0 \times 10^{-6}$ cm/s and $D_p = 16.16 \times 10^{-9}$ cm^2/s. These values of k_f and D_p are used to simulate the adsorption kinetics for different operating conditions. It is interesting to note that the estimated values of k_f and D_p are close to the values reported by McKay [2], i.e. $k_f = 80 \times 10^{-6}$ cm/s and $D_p = 18 \times 10^{-9}$ cm^2/s. The experimental observations and the model simulated concentration profiles for different initial dye concentrations, masses of silica and particle sizes of silica have been shown in Fig. 1b–d, respectively. From the above figures, it may be observed that beyond 120 min (2 h) of the process, the model under predicts the bulk concentration profile. This may be due to increase of the resistance inside the micropores which inhibits the process of adsorption.

(b) *Radke–Prausnitz isotherm* [3]: The system considered here is PNP—granular activated carbon from

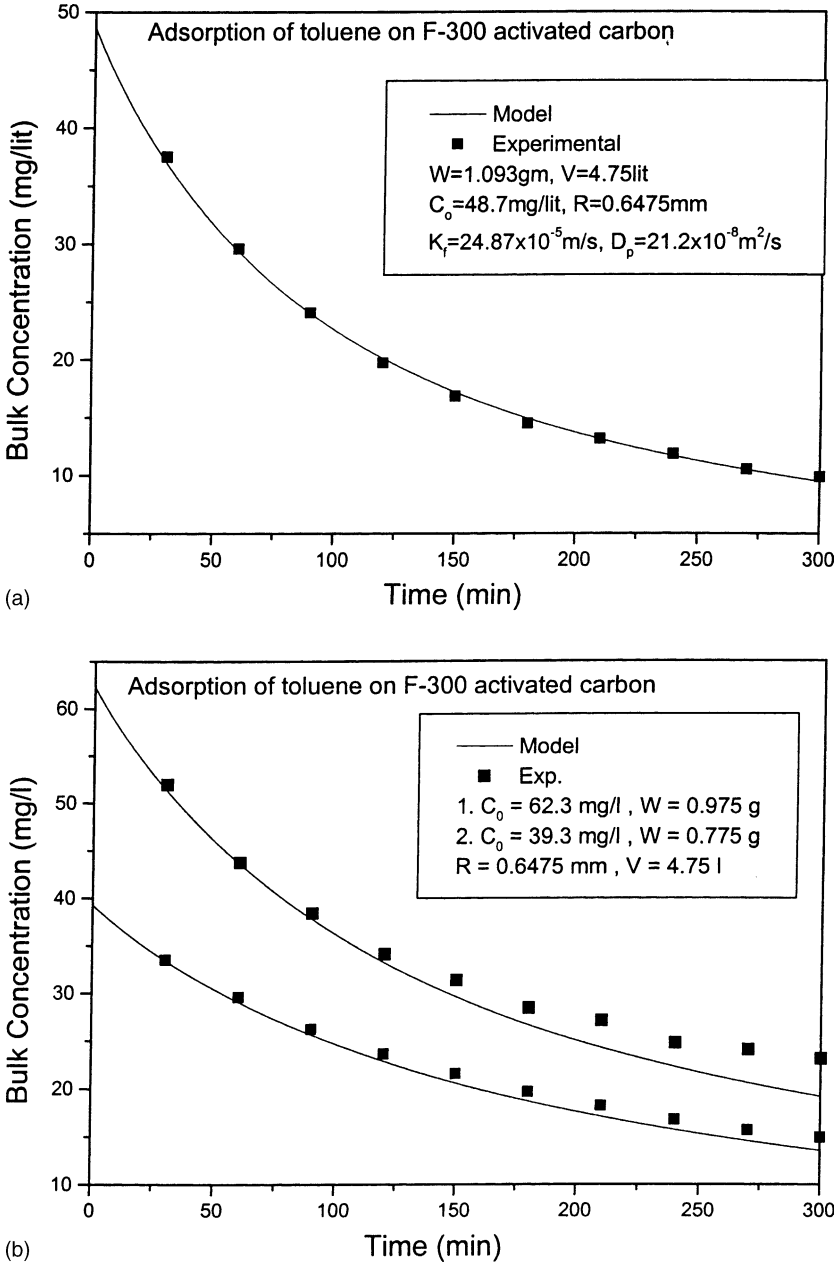

Fig. 3. (a) Adsorption of toluene; (b) effect of mass of adsorbent and initial adsorbate concentration.

Lurgi. The isotherm constants for three different temperatures are given (Table 1). It is clear from these results that the effect of temperature is pronounced well through the isotherm and also it affects the process parameters (k_f and D_p), which have been found out using the nonlinear parameter estimation. The values of the estimated parameters are given in Table 2.

Fig. 2 shows the model profile of concentration decay using the estimated parameters and the experimental data. It may be interesting to note that k_f varies almost linearly with temperature.

(c) *Fritz–Schlunder isotherm* [4]: The system considered here is toluene on F300 activated carbon. The isotherm constants are: $\alpha_1 = 120.03\,\text{mg/g}\,(\text{l/mg})^{-\beta_1}$, $\beta_1 = 0.5675$ and $\alpha_2 = 0.3060\,\text{mg/g}\,(\text{l/mg})^{-\beta_2}$, and $\beta_2 = 0.5955$. Where Y_e in mg/g and C_e in mg/l. For $C_0 = 48.7$ mg/l with $W = 39.3$ g, $V = 4.75$ l and particle size, $d = 1.295$ mm, the experimental data has been used to evaluate the unknown process parameters. The estimated values of the parameters are: $k_f = 24.87 \times 10^{-5}$ m/s and $D_p = 21.2 \times 10^{-8}\,\text{m}^2/\text{s}$. The fitting of data is presented in Fig. 3a.

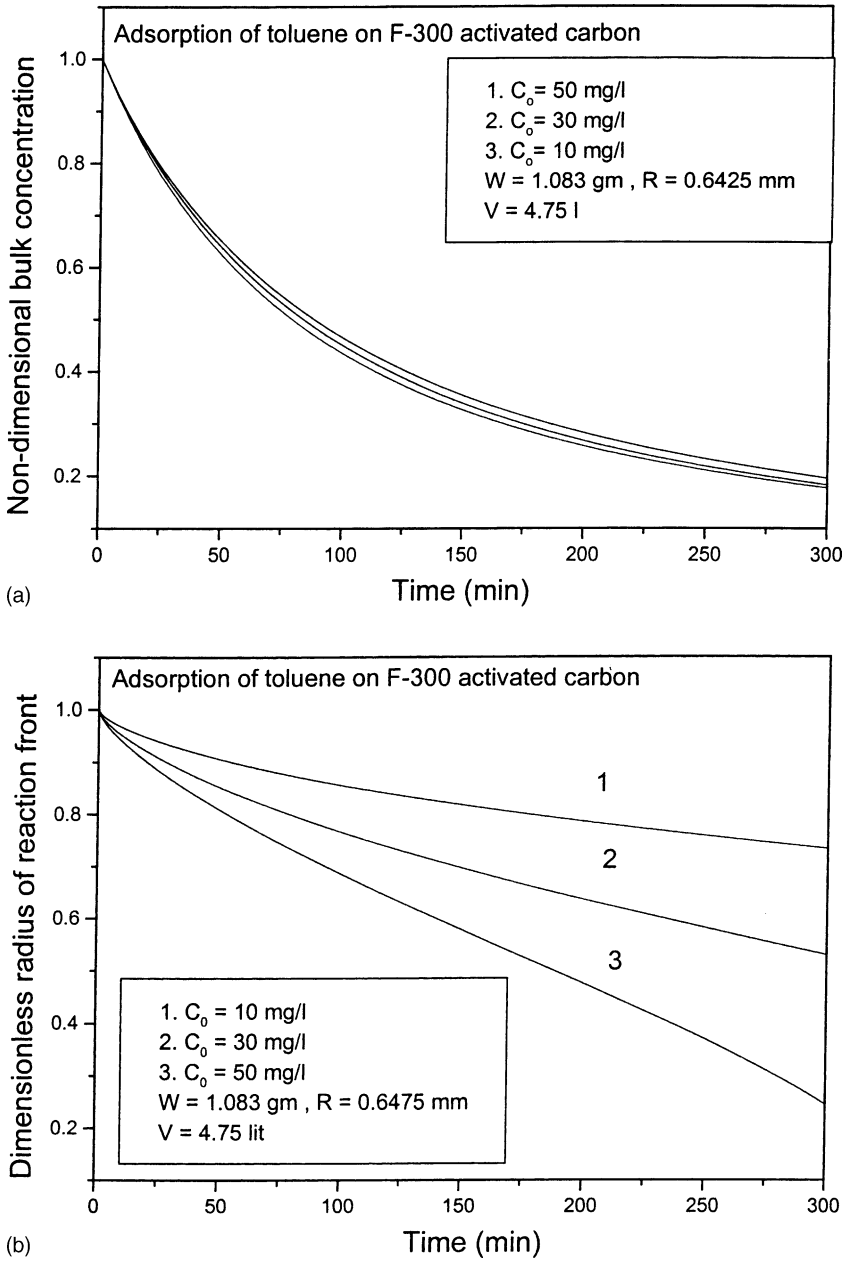

Fig. 4. (a) Effect of the initial adsorbate concentration on concentration decay; (b) effect of the initial adsorbate concentration on non-dimensional radius.

The estimated values of the parameters for the system, toluene on F300 activated carbon have been used to simulate the model for different initial toluene concentrations and masses of activated carbon. Fig. 3b shows that the concentration profile generated by the model is in excellent agreement with the experimental data for different initial concentrations and adsorbate dosages.

4.1. Parametric study

The various parameters that affect the adsorption kinetics are—the initial adsorbate concentration in liquid, the mass of adsorbent, the particle size of adsorbent, and the volume of the adsorbate solution, etc.

4.1.1. Effect of initial adsorbate concentration

With the decrease in initial adsorbate concentration in the solution, the rate of concentration decay in liquid phase increases, i.e. adsorption rate increases. It has been shown in Fig. 4a.

Fig. 4b shows that the decrease in non-dimensional radius (r) with time. The decrease in non-dimensional radius is more for higher initial adsorbate concentration. Therefore, the decrease in adsorption front is more for higher initial adsorbate concentration. Hence, the rate of adsorption

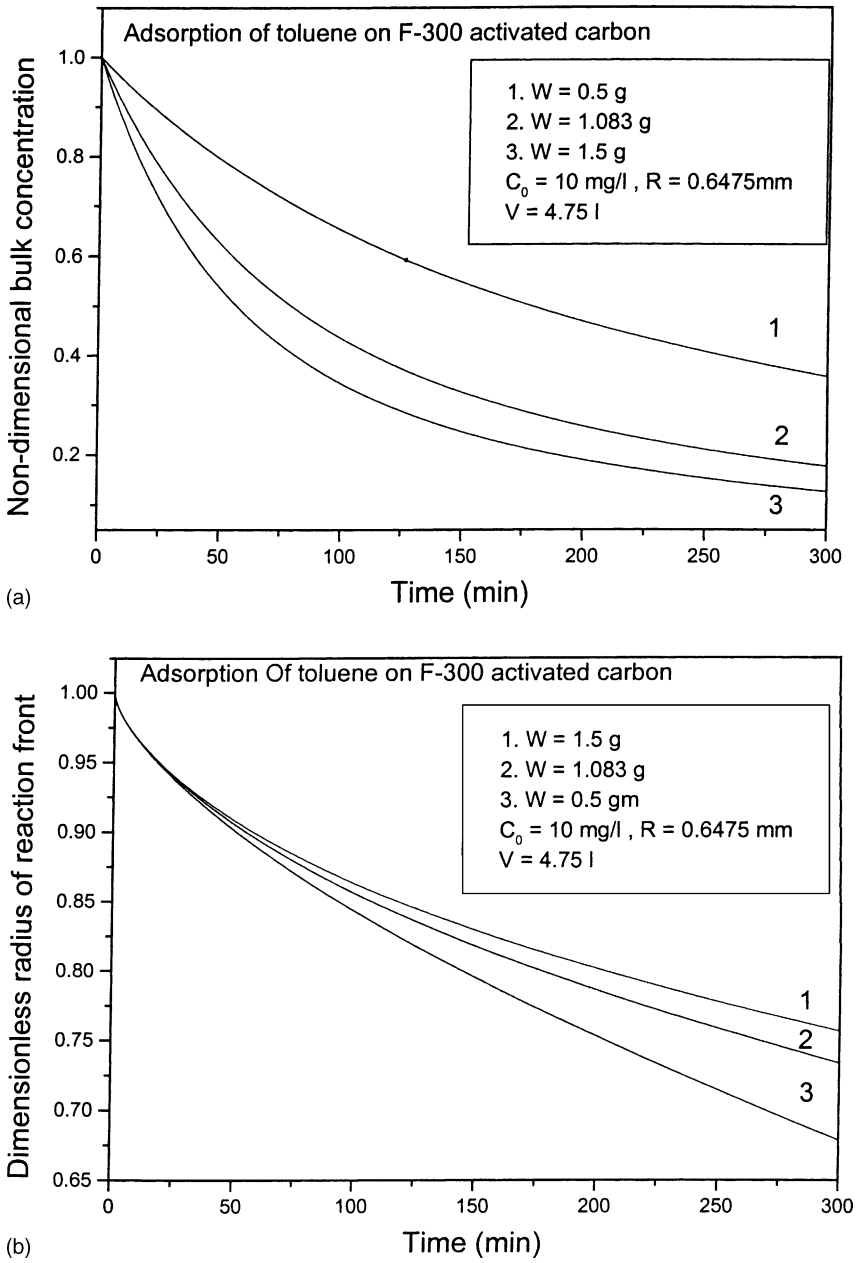

Fig. 5. (a) Effect of the mass of adsorbent on concentration decay; (b) effect of the mass of adsorbent on non-dimensional radius.

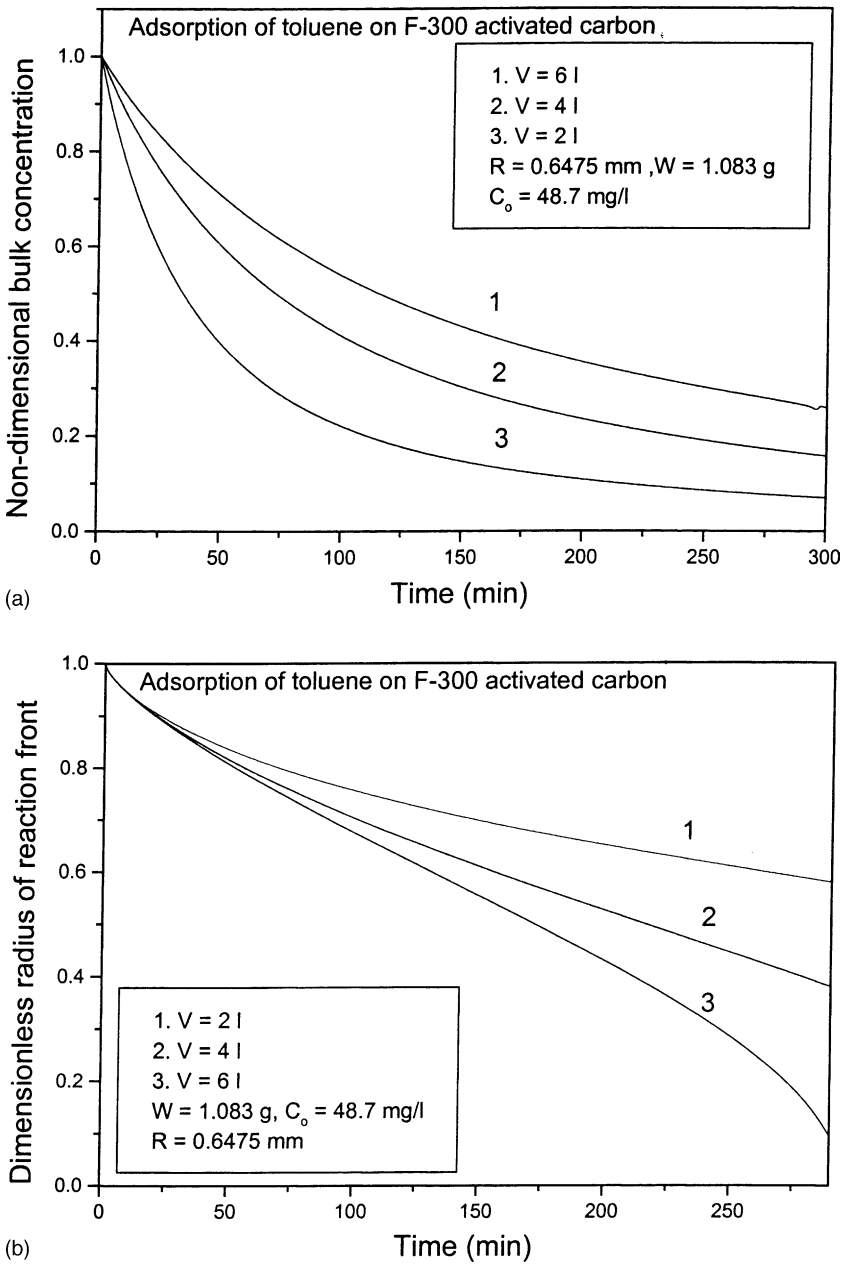

Fig. 6. (a) Effect of the volume of the adsorbate solution on concentration decay; (b) effect of the volume of adsorbate solution on non-dimensional radius.

decreases for higher initial adsorbate concentration. Therefore, it is evident that the adsorption process can be well represented by the rate of decrease of the unadsorbed portion of the adsorbent (in terms of dimensionless particle radius).

4.1.2. Effect of the mass of adsorbent

Fig. 5a shows the effect of mass of adsorbent on concentration decay in liquid phase. With the increase in mass of adsorbent, the adsorption sites increases. Therefore, the concentration decay in liquid phase increases.

Fig. 5b shows that the decrease in non-dimensional radius is less for higher mass of adsorbent. Therefore, the adsorption front for higher mass of adsorbent is more. Hence, the concentration decay is more for higher mass of adsorbent.

4.1.3. Effect of the volume of adsorbate solution

With the increase in volume of the adsorbate solution, the concentration decay in liquid phase decreases as shown in Fig. 6a. However, the decrease in non-dimensional radius (Fig. 6b) is more for higher volume of the adsorbate concentration, which explains the decrease in

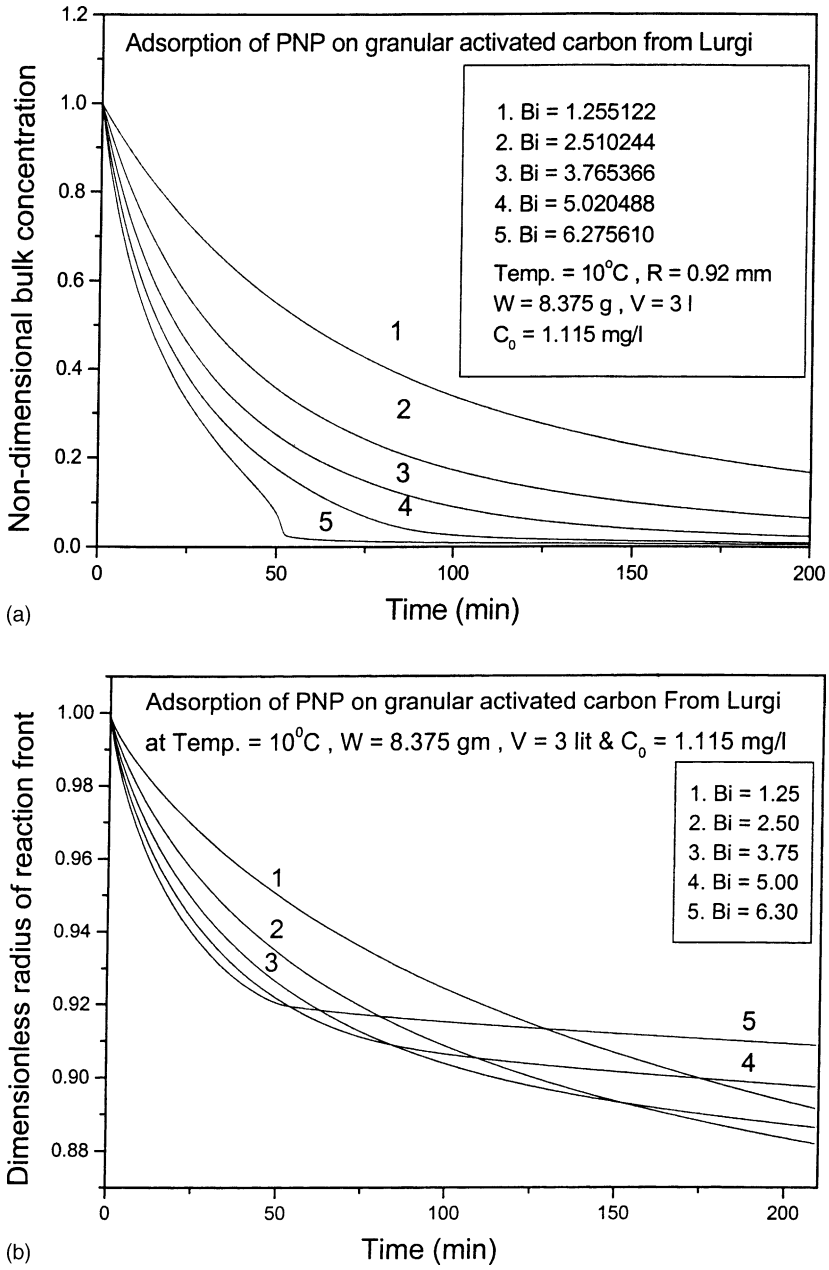

Fig. 7. (a) Effect of the Biot number on concentration decay; (b) effect of the Biot number on non-dimensional radius.

concentration decay with increase in volume of adsorbate solution.

4.1.4. Effect of the Biot number (Bi)

k_f, D_p, R, or their combinations can change the Biot number for a system. With constant D_p and R values, for different external mass transfer coefficient values, the model is simulated to observe the effect of Biot number on the concentration decay as shown in Fig. 7a. The figure shows that with increase in Biot number, the rate of concentration decay increases.

Fig. 7b shows that for the initial period of time, the decrease in the non-dimensional radius (r) is more for higher Biot number. So the external mass transfer coefficient is predominant in the initial period of time.

4.1.5. Effect of the adsorbent particle size

The rate of adsorption increases with the decrease of the adsorbent particle size. Fig. 8a and b show the effect of the adsorbent particle size on the non-dimensional concentration and the non-dimensional radius, respectively. With smaller particle size, the outer surface area is more for constant mass of adsorbent. Therefore, the adsorption front progresses rapidly with smaller particle size of adsorbent. Moreover, the rate of decrease of the non-dimensional radius is less for smaller particle size of the adsorbent.

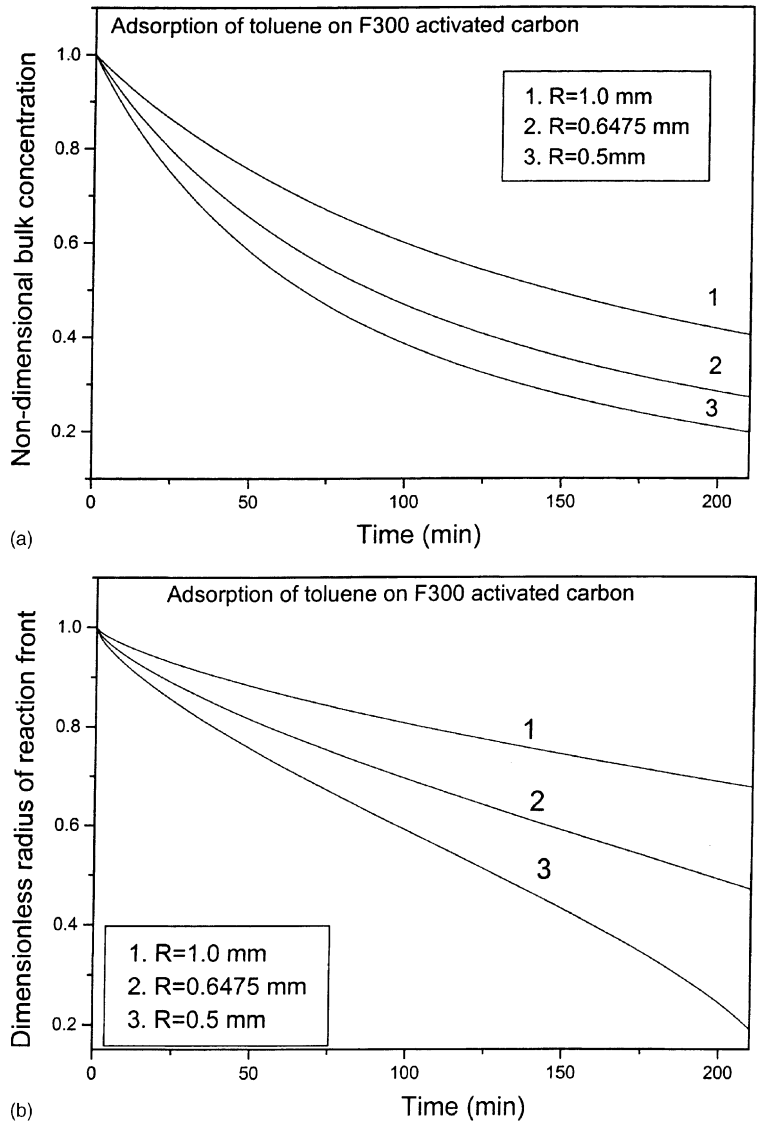

Fig. 8. (a) Effect of adsorbent particle size on concentration decay; (b) effect of the adsorbent particle size on non-dimensional radius.

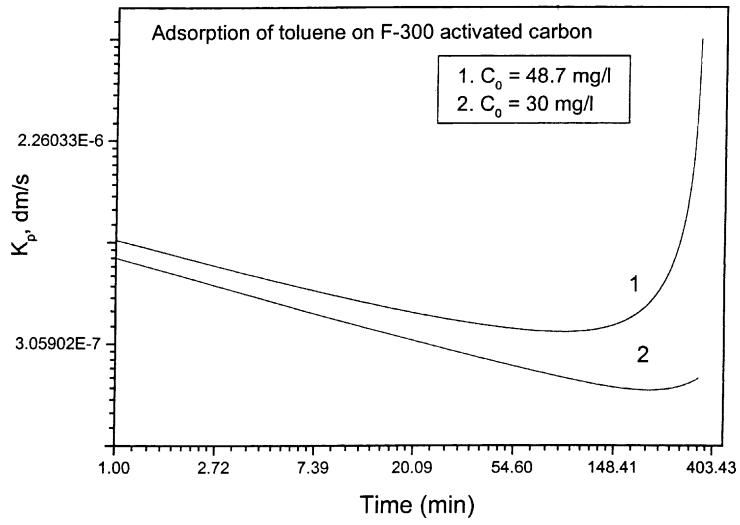

Fig. 9. Effect of initial toluene concentration on k_p.

4.1.6. Internal mass transfer coefficient

The mass transfer within the silica particle through the pores can be written as $N(t) = k_p A(Y_e - Y_t)$. Therefore, by comparing this equation with Eq. (4), the time dependent internal mass transfer coefficient is determined. Fig. 9 shows the value of k_p for initial adsorbate concentration. In case of homogeneous solid phase diffusion, k_p is proportional to the square root of adsorption time. However for the concerned system (toluene on F300 activated carbon), k_p values do not follow the ordinary diffusion laws for homogeneous particles as it is observed for the Astrazone Blue Dye on Silica [2].

5. Conclusion

The present pore diffusion model based on shrinking core formulation is a more generalized one, can be used for a wider range of initial adsorabate concentrations with all possible types of isotherms. The rate of adsorption increases with decrease in initial adsorbate concentration, increase in mass of adsorbent, decrease in adsorbent particle size, decrease in volume of adsorbate solution, and increase in temperature. It has also been observed from this study that the extent of adsorption can successfully be explained by the rate of decrease of the unadsorbed portion of the adsorbent (in terms of dimensionless particle radius). The effect of temperature is felt through the equilibrium isotherm and also the process parameters (k_f and D_p). The present model can be used for multicomponent adsorption processes and also with concentration dependent diffusivity. The model is useful to estimate k_f and D_p values, which are required for the design of fixed bed adsorber.

References

[1] C. Dimitrios, A. Verma, R.L. Irvine, Activated carbon adsorption and desorption of toluene in the aqueous phase, AIChE J. 39 (1993) 2027.
[2] G. McKay, Analytical solution using a pore diffusion model for the adsorption of basic dye on silica, AIChE J. 30 (1984) 692.
[3] E. Costa, G. Calleja, L. Marijuan, Adsorption of phenol and *p*-nitrophenol on activated carbon: determination of effective diffusion coefficient, Adsorp. Sci. Technol. 4 (1987) 58.
[4] C. Yen, P.C. Singer, Competitive adsorption of phenols on activated carbon, J. Environ. Eng. 110 (1984) 976.
[5] P. Mathews, W.J. Weber Jr., Effects of external mass transfer and intraparticle diffusion on adsorption rates in slurry reactors, in: Physical, Chemical Wastewater Treatment, vol. 91, AIChE Symp. Ser. Water, 1976.
[6] H. Komiyama, J. Smith, Surface diffusion in liquid filled pores, AIChE J. 20 (6) (1974) 1110.
[7] A.I. Liapis, D.W.T. Rippin, A general model for the simulation of multicomponent adsorption from a finite batch, Chem. Eng. Sci. 23 (1977) 619.
[8] T. Furusawa, J.M. Smith, Fluid-particle and intraparticle mass transport rates in sluries, Ind. Eng. Chem. Fundam. 12 (1973) 235.
[9] R.L. Dedrick, R.B. Beckmann, Kinetics of adsorption by activated carbon from dilute aqueous solution, AIChE. Symp. Ser. 74 (1967) 68.
[10] W.J. Weber Jr., R.R. Rumer, Intraparticle transport of sulfonated alkylbenzenes in a porous solid: diffusion and non-linear adsorption, Water Resour. Res. 1 (1965) 361.
[11] G. McKay, B. Al Duri, Multicomponent dye adsorption onto carbon using a solid diffusion mass-transfer model, Ind. Eng. Chem. Res. 30 (1991) 385.
[12] D.W. Hand, J.E. Crittenden, W.E. Thacker, User oriented batch reactor solutions to the homogeneous surface diffusion model, J. Environ. Eng. 109 (1983) 82.
[13] A. Kapoor, R.T. Yang, C. Wong, Surface diffusion, Catal. Rev. Sci. Eng. 31 (1989) 129.
[14] O. Levenspiel, Chemical Reaction Engineering, 2nd ed., Wiley, New York, 1972.
[15] C.Y. Wen, Non-catalytic heterogeneous solid–fluid reaction models, Ind. Eng. Chem. 60 (1968) 34.
[16] I. Neretnieks, Adsorption in finite batch and counter flow with systems having a nonlinear isotherm, Chem. Eng. Sci. 131 (1976) 107.
[17] H. Spahn, E.U. Schlunder, The scale-up of activated carbon columns for water purification based on batch tests I, Chem. Eng. Sci. 30 (1975) 529.
[18] H.S. Fogler, Elements of Chemical Reaction Engineering, 2nd ed., Prentice-Hall, New Delhi, India, 1997.